

Synthesis and Solution Characterization of $[\text{Ru}(\text{bpy})_2]^{2+}$ Modified Polyazines

Meng Cheng and William B. Euler*

Department of Chemistry, 51 Lower College Road, University of Rhode Island, Kingston, Rhode Island 02881

Received March 20, 2003; Revised Manuscript Received June 20, 2003

A series of $[\text{Ru}(\text{bpy})_2]^{2+}$ complexes linked by a controlled number of azine units (one to seven) were synthesized and studied in the solution phase. Polymers and dimer model compounds were examined by cyclic voltammetry and IR, NMR, and visible-NIR spectroscopies. The NMR spectra and the cyclic voltammograms indicated that the Ru^{2+} sites influenced the main chain properties at least 15 Å from the metal site. The first oxidation in each material was assigned to a ligand-centered process, but DFT calculations suggested that the Ru^{2+} has an important influence. The first oxidized state of the polymers has a spectroscopic band that is consistent with an intervalence transfer (IT) transition, but this absorption is not seen in the dimer model compounds. Thus, the IT feature is assigned to a ligand–ligand transition that spans several repeat units in the polymer.

Introduction

The study of the electron-transfer properties of dimetal Ru^{2+} complexes has had a long history.^{1–6} These types of complexes have been shown to have ideal properties to study theories of charge-transfer, and work continues to refine our understanding of the role of the geometry in determining the interaction between metal sites, including both distance^{7–25}

and angular parameters.^{26–35} In general, the coupling between metal sites is strongest when the interacting orbitals are parallel and as close to each other as possible.

More recently, oligomeric and polymeric complexes containing Ru^{2+} and other metal ions have been investigated.^{36–52} Such systems may allow directed transport along

* Author to whom correspondence should be addressed. E-mail: weuler@chm.uri.edu.

- (1) Hush, N. S. *Prog. Inorg. Chem.* **1967**, *8*, 391.
- (2) Sutin, N. *Acc. Chem. Res.* **1982**, *15*, 275.
- (3) Creutz, C. *Prog. Inorg. Chem.* **1983**, *30*, 1.
- (4) Sutin, N. *Prog. Inorg. Chem.* **1983**, *30*, 441.
- (5) Endicott, J. F.; Watzky, M. A.; Song, X.; Buranda, T. *Coord. Chem. Rev.* **1997**, *159*, 295.
- (6) Demadis, K. D.; Hartshorn, C. M.; Meyer, T. J. *Chem. Rev.* **2001**, *101*, 2655.
- (7) Collin, J.-P.; Lainé, P.; Launay, J.-P.; Sauvage, J.-P.; Sour, A. *J. Chem. Soc. Chem. Commun.* **1993**, 434.
- (8) Salaymeh, F.; Berhame, S.; Yusof, R.; de la Rosa, R.; Fung, E. Y.; Matamoros, R.; Lau, K. W.; Zheng, Q.; Kober, E. M.; Curtis, J. C. *Inorg. Chem.* **1993**, *32*, 3895.
- (9) Barigelletti, L.; Flamigni, L.; Balzani, V.; Collin, J.-P.; Sauvage, J.-P.; Sour, A.; Constable, E. C. *J. Am. Chem. Soc.* **1994**, *116*, 7692.
- (10) Reimers, J. R.; Hush, N. S. *J. Am. Chem. Soc.* **1995**, *117*, 1302.
- (11) Kelso, L. S.; Reitsma, D. A.; Keene, F. R. *Inorg. Chem.* **1996**, *35*, 5144.
- (12) Elliot, C. M.; Derr, D. L.; Ferrere, S.; Newton, M. D.; Liu, Y.-P. *J. Am. Chem. Soc.* **1996**, *118*, 5221.
- (13) Ward, M. D. *Inorg. Chem.* **1996**, *35*, 1712.
- (14) Elliott, C. M.; Derr, D. L.; Matyushov, D. V.; Newton, M. D. *J. Am. Chem. Soc.* **1998**, *120*, 11714.
- (15) Baitalik, S.; Flörke, U.; Nag, K. *Inorg. Chem.* **1999**, *38*, 3296.
- (16) Glöckle, M.; Kaim, W.; Katz, N. E.; Posse, M. G.; Cutin, E. H.; Fiedler, J. *Inorg. Chem.* **1999**, *38*, 3270.

- (17) Encinas, S.; Barthram, A. M.; Ward, M. D.; Barigelletti, F.; Campagna, S. *Chem. Commun.* **2001**, 277.
- (18) Pappenfuss, T. M.; Mann, K. R. *Inorg. Chem.* **2001**, *40*, 6301.
- (19) D'Alessandro, D. M.; Kelso, L. S.; Keene, F. R. *Inorg. Chem.* **2001**, *40*, 6841.
- (20) Seneviratne, D. S.; Uddin, M. J.; Swayambunathan, V.; Schlegel, H. B.; Endicott, J. F. *Inorg. Chem.* **2002**, *41*, 1502.
- (21) Oh, D.; Boxer, S. G. *J. Am. Chem. Soc.* **1990**, *112*, 8161.
- (22) Hupp, J. T.; Dong, Y.; Blackburn, R. L.; Lu, H. *J. Phys. Chem.* **1993**, *97*, 3278.
- (23) Karki, L.; Lu, H. P.; Hupp, J. T. *J. Phys. Chem.* **1996**, *100*, 15637.
- (24) Cave, R. J.; Newton, M. D. *J. Chem. Phys.* **1997**, *106*, 9213.
- (25) Nelsen, S. F.; Newton, M. D. *J. Phys. Chem. A* **2000**, *104*, 10023.
- (26) Siders, P.; Cave, R. J.; Marcus, R. A. *J. Chem. Phys.* **1984**, *81*, 5613.
- (27) Cave, R. J.; Siders, P.; Marcus, R. A. *J. Phys. Chem.* **1986**, *90*, 1436.
- (28) Ohta, K.; Closs, G. L.; Morokuma, K.; Green, N. J. *J. Am. Chem. Soc.* **1986**, *108*, 1319.
- (29) Sessler, J.; Johnson, M.; Lin, T. Y.; Creager, S. *J. Am. Chem. Soc.* **1988**, *110*, 3659.
- (30) Osuka, A.; Maruyama, K.; Mataga, N.; Asahi, T.; Yamazaki, I.; Tamai, N. *J. Am. Chem. Soc.* **1990**, *112*, 4958.
- (31) Helms, A.; Heiler, D.; McLendon, G. *J. Am. Chem. Soc.* **1991**, *113*, 4325.
- (32) Helms, A.; Heiler, D.; McLendon, G. *J. Am. Chem. Soc.* **1992**, *114*, 6227.
- (33) Paddon-Row, M. N.; Shephard, M. J.; Jordan, K. D. *J. Am. Chem. Soc.* **1993**, *115*, 3312.
- (34) Lewis, N. A.; Pan, W. *Inorg. Chem.* **1995**, *34*, 2244.
- (35) Metcalfe, R. A.; Dodsworth, E. S.; Fiedler, S. S.; Stufkens, D. J.; Lever, A. B. P.; Pietro, W. J. *Inorg. Chem.* **1996**, *35*, 7741.

the macromolecular backbone or provide amplification of chiral or optical behavior.^{53–59} This is particularly interesting if the polymeric system is conjugated so that charge transport may occur either directly from metal-to-metal or along the delocalized polymer chain.

Our interests have been in the polyazine family of polymers, $-\text{N}=\text{C}(\text{R})-\text{C}(\text{R})=\text{N}-$.^{60–65} The diimine site in the polymer is ideal for binding to metal ions, so we^{39,66} and others^{67–69} have been studying metal complexes containing this diimine unit. The purely organic polyazines are conjugated but only modestly delocalized and do not readily oxidize with mild reagents such as I₂. For those oligoazines and polyazines that can be dissolved in organic solvents, NMR evidence shows multiple conformations in solution that are attributed to the low energy costs for rotations about the

N–N bond.⁶⁵ Despite this, under solution conditions the conjugation length of the polyazine is on the order of 8–10 double bonds. This combination of properties leads to a band gap of 3.3 eV for the polyazines.

Even though the N–N bonds are conformationally labile, the C–C bonds are rigid and in the *s-trans* conformation in polyazines. This means that direct complexation of metal ions to the diimine unit is not energetically feasible. To form complexes of polyazines, monomer complexes must be prepared first and then condensed into the polymer.³⁹ We have previously⁶⁶ studied a variety of Ru²⁺ complexes that contain azine units, including [Ru(bpy)₂BDDH]²⁺ (bpy = 2,2'-bipyridine and BDDH = 2,3-butanedione dihydrazone) and [Ru(bpy)₂BADA]²⁺ (BADA = biacetyl diazine), which can both be used to form polyazines containing the Ru-(bpy)₂²⁺ complex. [Ru(bpy)₂BDDH]²⁺ and [Ru(bpy)₂BADA]²⁺ both are similar to [Ru(bpy)₃]²⁺ spectroscopically and electrochemically so are useful starting materials to build polymers that can be examined for comparison to the well-studied [Ru(bpy)₃]²⁺. In this paper, we report our initial synthesis and solution characterization (NMR, vis-NIR, cyclic voltammetry) of polyazines containing Ru(bpy)₂²⁺ substituent groups at well-defined intervals along the polymer backbone. For comparison purposes, we also synthesized a number of dimer model compounds.

The presence of the metal complex has remarkable effects on the physical and chemical properties of the polyazines. The polymer complexes become water-soluble, and the ligand is oxidized at low potentials. The ligand can be reversibly oxidized as long as the Ru²⁺ is not oxidized, but formation of Ru³⁺ induces rearrangement of the polymer structure. The influence of the Ru²⁺ ions is long range, extending at least 15 Å down the polymer chain, as indicated by both the electrochemical potentials and the NMR chemical shifts. Oxidation of the polymers leads to an intervalence transfer (IT) band in the NIR that is not found in oxidized dimers. This suggests that the IT absorption is associated with an intraligand, dimer-to-dimer transition. We support our conclusions using PM3 and DFT calculations. The geometries found by the PM3 calculations suggest that the polyazine backbone is significantly twisted, leading to a helical polymer. The DFT calculations confirm that the first oxidation should be ligand based and that there is substantial delocalization of the oxidation.

Experimental Section

Reagents and Chemicals. Ru(BADA)(bipy)₂(PF₆)₂ and Ru-(BDDH)(bipy)₂(PF₆)₂ were synthesized according to previously published methods.⁶⁶ All the bridging ligands were prepared by literature methods.^{60,65} Acetonitrile was purchased from Aldrich, and acetic acid was purchased from Fisher.

Dimer Syntheses. Dimer2 was prepared by reacting 95.4 mg (0.1 mmol) [Ru(bpy)₂BADA](PF₆)₂ with 2.43 μL (0.05 mmol) of hydrazine hydrate (NH₂NH₂·H₂O) in 20 mL of 3:1 (v/v) acetonitrile/acetic acid. The mixture was stirred and heated at 75 °C under nitrogen for 15 days. The reaction solution was then filtered, and the filtrate was rotary evaporated to remove the solvent (hexane can be added to help the removal of acetic acid). The sticky liquid was transferred to a thimble and Soxhlet extracted with dichlo-

- (36) Brown, G. M.; Meyer, T. J.; Cowan, D. O.; LeVanda, C.; Kaufman, F.; Roling, P. V.; Rausch, M. D. *Inorg. Chem.* **1975**, *14*, 506.
- (37) Powers, M. J.; Callahan, R. W.; Salmon, D. J.; Meyer, T. J. *Inorg. Chem.* **1976**, *15*, 894.
- (38) Von Kameke, A.; Tom, G. M.; Taube, H. *Inorg. Chem.* **1978**, *17*, 1790.
- (39) Euler, W. B. *Polyhedron* **1991**, *10*, 859.
- (40) Adams, C. J.; James, S. L.; Raithby, P. R. *Chem. Commun.* **1997**, 2155.
- (41) Ley, K. D.; Whittle, C. E.; Bartberger, M. D.; Schanze, K. S. *J. Am. Chem. Soc.* **1997**, *119*, 3423.
- (42) Zhu, S. S.; Kingsborough, R. P.; Swager, T. M. *J. Mater. Chem.* **1999**, *9*, 2123.
- (43) Macatangay, A. V.; Mazzetto, S. E.; Endicott, J. F. *Inorg. Chem.* **1999**, *38*, 5091.
- (44) Ley, K. D.; Li, Y.; Johnson, J. V.; Powell, D. H.; Schanze, K. S. *Chem. Commun.* **1999**, 1749–1750.
- (45) Macatangay, A. V.; Endicott, J. F. *Inorg. Chem.* **2000**, *39*, 437.
- (46) Walters, K. A.; Trouillet, L.; Guillerez, S.; Schanze, K. S. *Inorg. Chem.* **2000**, *39*, 5496.
- (47) Trouillet, L.; De Nicola, A.; Guillerez, S. *Chem. Mater.* **2000**, *12*, 1611.
- (48) Wang, Q.; Yu, L. *J. Am. Chem. Soc.* **2000**, *122*, 11806.
- (49) Manners, I. *Science* **2001**, *294*, 1664.
- (50) Pappenfuss, T. M.; Mann, K. R. *Inorg. Chem.* **2001**, *40*, 6301.
- (51) Serin, J.; Schultze, X.; Adronov, A.; Fréchet, J. M. J. *Macromolecules* **2002**, *35*, 5396.
- (52) Sommovigo, M.; Ferretti, A.; Venturi, M.; Ceroni, P.; Giardi, C.; Denti, G. *Inorg. Chem.* **2002**, *41*, 1263.
- (53) Green, M. M.; Andreola, C.; Munoz, B.; Reidy, M. P.; Zero, K. *J. Am. Chem. Soc.* **1988**, *110*, 4063.
- (54) Lifson, S.; Andreola, C.; Peterson, N. C.; Green, M. M. *J. Am. Chem. Soc.* **1989**, *111*, 8850.
- (55) Green, M. M.; Reidy, M. P.; Johnson, R. D.; Darling, G.; O'Leary, D. J.; Willson, G. *J. Am. Chem. Soc.* **1989**, *111*, 6452.
- (56) Green, M. M.; Khatri, C.; Peterson, N. C. *J. Am. Chem. Soc.* **1993**, *115*, 4941.
- (57) Gu, H.; Nakamura, Y.; Sato, T.; Teramoto, A.; Green, M. M.; Jha, S. K.; Andreola, C.; Ready, M. P. *Macromolecules* **1998**, *31*, 6362.
- (58) Levitsky, I. A.; Kishikawa, K.; Eichorn, S. H.; Swager, T. M. *J. Am. Chem. Soc.* **2000**, *122*, 2474.
- (59) Galoppini, E.; Guo, W.; Zhang, W.; Hoertz, P. G.; Qu, P.; Meyer, G. *J. Am. Chem. Soc.* **2002**, *124*, 7801–7811.
- (60) Hauer, C. R.; King, G. S.; McCool, E. L.; Euler, W. B.; Ferrara, J. D.; Youngs, W. J. *J. Am. Chem. Soc.* **1987**, *109*, 5760.
- (61) Chaloner-Gill, B.; Euler, W. B.; Mumbauer, P. D.; Roberts, J. E. *J. Am. Chem. Soc.* **1991**, *113*, 6831.
- (62) Euler, W. B. *Chem. Mater.* **1996**, *8*, 554.
- (63) Euler, W. B. *Handbook of Organic Conductive Molecules and Polymers*; H. S. Nalwa, Ed., John Wiley & Sons: Chichester, 1997, Vol. 2, 719.
- (64) Kessler, E. C.; Euler, W. B.; Foxman, B. M. *Chem. Mater.* **1999**, *11*, 336.
- (65) Euler, W. B.; Cheng, M.; Zhao, C. *Chem. Mater.* **1999**, *11*, 3702.
- (66) Euler, W. B.; Cheng, M.; Zhao, C. *Polyhedron* **2001**, *20*, 507.
- (67) Rasmussen, S. C.; Thompson, D. W.; Singh, V.; Peterson, J. D. *Inorg. Chem.* **1996**, *35*, 3449.
- (68) Lewis, M.; Glaser, R. *J. Org. Chem.* **2002**, *67*, 1441.
- (69) Sauro, V. A.; Workentin, M. S. *J. Org. Chem.* **2001**, *66*, 831.

romethane for 2 days. The solution in the flask was collected and evaporated to get a deep red and sticky liquid. A deep red colored solid can be obtained after vacuum-drying. Yield 39.4 mg, 41%. IR: 3415, 2920, 2850, 1696, 1663, 1465, 1375, 1124, 1084, 772 cm^{-1} . ^1H NMR (DMSO- d_6): δ vs TMS, 0.80 (m), 1.75 (s), 1.83 (s), 2.07 (s), 2.46 (s), 8.06–9.67 (m, bpy). The other dimers were prepared analogously. Dimer3: 47.7 mg (0.05 mmol) of [Ru(bipy)₂BADA](PF₆)₂; 2.9 mg (0.025 mmol) of butanedione dihydrazone (C₄H₁₀N₄). Yield 19.6 mg, 38%. IR: 3405, 3196, 2925, 2851, 1701, 1669, 1457, 1384, 1262, 1084, 1029, 803, 771 cm^{-1} . ^1H NMR (DMSO- d_6): δ vs TMS, 0.87 (m), 1.23 (s), 1.75 (s), 1.83 (s), 2.07 (s), 8.06–9.67 (m, bpy). Dimer4: 47.7 mg (0.05 mmol) of [Ru(bipy)₂BADA](PF₆)₂; 4.9 mg (0.025 mmol) of diacetylazine dihydrazone (C₈H₁₆N₆). Yield 22.0 mg, 43%. IR: 3433, 3193, 2921, 2850, 1690, 1465, 1375, 1273, 1123, 1084, 772 cm^{-1} . ^1H NMR (DMSO- d_6): δ vs TMS, 0.86 (m), 1.24 (s), 1.85 (s), 2.07 (s), 8.06–9.67 (m, bpy). Dimer5: 47.7 mg (0.05 mmol) of [Ru(bipy)₂BADA](PF₆)₂; 6.9 mg (0.025 mmol) of C₁₂H₂₂N₈. Yield 18.6 mg, 35%. IR: 3372, 3143, 2918, 2850, 1696, 1646, 1457, 1402, 1125, 1084, 770 cm^{-1} . ^1H NMR (DMSO- d_6): δ vs TMS, 0.86 (m), 1.23 (s), 1.75 (s), 1.86 (s), 8.06–9.67 (m, bpy). Dimer6: 47.7 mg (0.05 mmol) of [Ru(bipy)₂BADA](PF₆)₂; 9.0 mg (0.025 mmol) of C₁₆H₂₈N₁₀. Yield 20.0 mg, 36%. IR: 3351, 3181, 2925, 2852, 1672, 1445, 1392, 1265, 1125, 1084, 772 cm^{-1} . ^1H NMR (DMSO- d_6): δ vs TMS, 0.86 (m), 1.24 (s), 1.76 (s), 1.84 (s), 8.06–9.67 (m, bpy).

Polymer Syntheses. Poly1 was prepared by reacting 47.7 mg (0.05 mmol) of [Ru(bipy)₂BADA](PF₆)₂ with 40.9 mg (0.05 mmol) of [Ru(bipy)₂BDDH](PF₆)₂ in 20 mL of 3:1 (v/v) acetonitrile/acetic acid. The mixture was stirred and heated at 75 °C under nitrogen for 28 days. The reaction solution was then filtered, and the filtrate was rotary evaporated to remove the solvent (hexane can be added to help the removal of acetic acid). The sticky liquid was transferred to a thimble and Soxhlet extracted with dichloromethane for 2 days. The solution in the flask was collected and evaporated to get a deep red and sticky liquid. A deep red colored solid can be obtained after vacuum-drying. Yield 18.6 mg, 21%. IR: 3436, 2923, 2854, 1707, 1457, 1378, 1125, 1084, 769 cm^{-1} . ^1H NMR (DMSO- d_6): δ 0.86 (br), 1.239, 7.2–9.7 (unresolved, bpy). The other polymers were prepared analogously. Poly2: 47.7 mg (0.05 mmol) of [Ru(bipy)₂BADA](PF₆)₂; 2.43 μL (0.05 mmol) of hydrazine hydrate (NH₂NH₂·H₂O), 15 days' reaction time. Yield 16.7 mg, 35%. IR: 3391, 3188, 2917, 2851, 1703, 1665, 1603, 1463, 1377, 1122, 1084, 772, 743 cm^{-1} . ^1H NMR (DMSO- d_6): δ 0.85 (br), 1.239, 1.756, 1.835, 2.081, 7.2–9.0 (unresolved, bpy). Poly3: 47.7 mg (0.05 mmol) of [Ru(bipy)₂BADA](PF₆)₂ with 5.7 mg (0.05 mmol) of butanedione dihydrazone (C₄H₁₀N₄), 15 days' reaction time. Yield 19.6 mg, 38%. IR: 3415, 2922, 2852, 1669, 1465, 1384, 1124, 1084, 771 cm^{-1} . ^1H NMR (DMSO- d_6): δ 0.86 (br), 1.237, 1.759, 1.836, 2.191, 7.2–9.0 (unresolved, bpy). Poly4: 47.7 mg (0.05 mmol) of [Ru(bipy)₂BADA](PF₆)₂; 9.8 mg (0.05 mmol) of acetylazine dihydrazone (C₈H₁₆N₆), 15 days' reaction time. Yield 22.8 mg, 41%. IR: 3404, 3197, 2925, 2852, 1690, 1669, 1465, 1385, 1122, 1084, 1031, 803, 771 cm^{-1} . ^1H NMR (DMSO- d_6): δ 0.87 (br), 1.243, 1.758, 1.837, 2.081, 7.2–9.0 (unresolved, bpy). Poly5: 47.7 mg (0.05 mmol) of [Ru(bipy)₂BADA](PF₆)₂ with 13.9 mg (0.05 mmol) of C₁₂H₂₂N₈, 15 days' reaction time. Yield 22.1 mg, 37%. IR: 3421, 3206, 2923, 2850, 1701, 1663, 1465, 1384, 1124, 1084, 772 cm^{-1} . ^1H NMR (DMSO- d_6): δ 0.88 (br), 1.240, 1.756, 1.835, 2.078, 7.2–9.0 (unresolved, bpy). Poly6: 47.7 mg (0.05 mmol) of [Ru(bipy)₂BADA](PF₆)₂; 18.0 mg (0.05 mmol) of C₁₆H₂₈N₁₀, 15 days' reaction time. Yield 26.8 mg, 42%. IR: 3438, 2922, 2850, 1670, 1457, 1384, 1124, 1084, 842, 772 cm^{-1} . ^1H NMR (DMSO- d_6): δ 0.87 (br), 1.240, 1.836, 2.079, 7.2–9.0 (unresolved,

bpy). Poly7: 47.7 mg (0.05 mmol) of [Ru(bipy)₂BADA](PF₆)₂; 22.1 mg of (0.05 mmol) C₂₀H₃₄N₁₂, 15 days' reaction time. Yield 24.4 mg, 36%. IR: 3351, 3216, 2923, 2850, 1707, 1663, 1465, 1384, 1264, 1124, 1084, 772 cm^{-1} . ^1H NMR (DMSO- d_6): δ 0.86 (br), 1.239, 1.754, 1.836, 2.071, 7.2–9.0 (unresolved, bpy).

Measurements. IR spectra were measured as KBr pellets on a Perkin-Elmer model 1650 FTIR spectrometer at 2 cm^{-1} resolution between 450 and 4000 cm^{-1} . ^1H NMR spectra were obtained in DMSO- d_6 at room temperature on a JEOL Eclipse 400 spectrometer at 400 MHz and are referenced against TMS. UV–vis–NIR spectra were obtained in acetonitrile on a Perkin-Elmer Lambda 900 spectrometer. Spectra were deconvoluted using the fitting routines in SigmaPlot v5.0. Oxidation titrations were typically done using 0.01 M ceric ammonium nitrate and 10^{−4} M [Ru²⁺] (accurately measured) dissolved in acetonitrile; spectra were measured after each addition of 2 μL of oxidant in a cell with total initial volume of polymer solution of 2.0 mL. Emission spectra were measured using a Spex Fluorolog spectrometer in nitrogen degassed acetonitrile at room temperature. Cyclic voltammetry was run using a BioAnalytical Systems CV-27 with a platinum button working electrode, platinum wire counter electrode, a Ag/AgCl reference electrode in a 0.1 M LiClO₄ acetonitrile solution at 25 °C using a scan rate of 100 mV/s.

Theoretical calculations were run using Spartan 02 (Build 114) for Linux 2.2⁷⁰ Geometries were optimized using the PM3 method.⁷¹ No negative frequencies were found, indicating that the structures were minima. The presence of the ruthenium ion requires the use of the PM3 method, but our previous work has shown that AM1 and PM3 give similar geometries for polyazines.^{64,65} Using the PM3 optimized geometry, the electronic structure was calculated using density functional theory using the B3LYP hybrid functional^{72,73} and the 3-21G* basis set.

Results

Synthesis. Polyazines are synthesized by condensation of a diketone with a dihydrazone.^{60–63} For the metal-containing polymers, direct reaction of a polyazine with a metal complex does not give reaction because the diimine linkage is in the *s-trans* conformation rather than the required *s-cis* conformation. To obtain the desired synthetic goal, the metal complex was synthesized followed by condensation to give the polymer. Two metal complexes could be used as monomers, one containing amine end groups or one containing ketone end groups. Both complexes have been synthesized, as previously reported,⁶⁶ by substitution of the chloride ligands in *cis*-[Ru(bpy)₂Cl₂] giving either [Ru(bpy)₂BDDH]²⁺ (NH₂ end groups) or [Ru(bpy)₂BADA]²⁺ (C=O end groups). For polymerization, we found that [Ru(bpy)₂BADA]²⁺ was significantly more reactive, so this monomer was used in all of the syntheses reported here, as shown in Scheme 1. We presume that the lower reactivity of [Ru(bpy)₂BDDH]²⁺ arises because of the reduced nucleophilicity of the amine groups near the cationic metal. The choice of comonomer allowed us to prepare materials with 1 (Poly1) to 7 (Poly7) azine spacers between metal sites. The nominal metal–metal

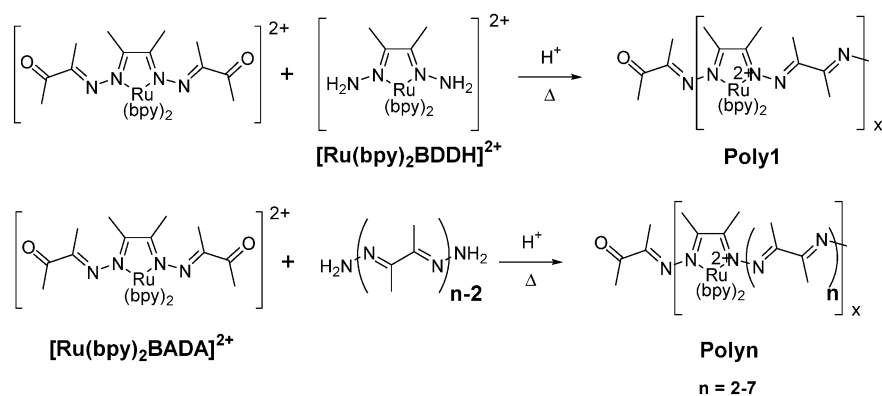
(70) Spartan for Linux, Wavefunction, Inc., 18401 Von Karman Ave., Ste. 370, Irvine, CA 92612 U.S.A.

(71) Stewart, J. J. P. *J. Comput. Chem.* **1989**, *10*, 209.

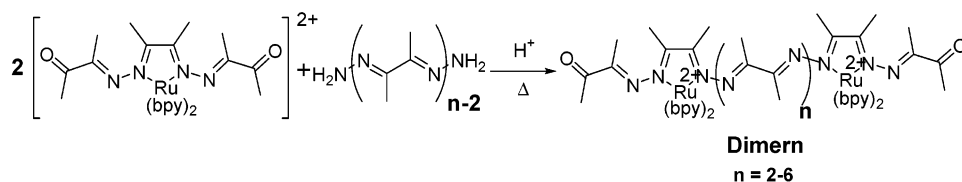
(72) Becke, A. D. *Phys. Rev. A* **1988**, *38*, 3098.

(73) Perdew, J. P. *Phys. Rev. B* **1986**, *33*, 8822.

Scheme 1



Scheme 2



distances in these polymers range from about 9 Å in Poly1 to about 32 Å in Poly7, based on molecular models.

In contrast to the purely organic polyazines, which are insoluble in all common solvents, the ruthenium-containing polymers are all hygroscopic and water soluble. All of the complexed polymers are also modestly soluble in polar solvents such as acetonitrile, DMSO, and methylene chloride but are not soluble in alcohols.

We also synthesized dimer model compounds by using stoichiometric control of the reactants, as shown in Scheme 2, with two (Dimer2) to six (Dimer6) azine units between metal sites. In principle, we should be able to make Dimer1 by reacting excess $[\text{Ru}(\text{bpy})_2\text{BDDH}]^{2+}$ with butanedione. However, this reaction was unsuccessful in all of our attempts.

IR Spectroscopy. The IR spectra for all of the dimers and polymers were consistent with the proposed structures. Organic polyazines typically have strong absorption bands near 1120, 1360, 1440, and 1600 cm^{-1} and weaker bands in the C–H stretching region below 3000 cm^{-1} .^{60–62} All of the materials synthesized here have bands at 1123(± 1), 1381(± 4), 1461(± 4), 1667 (± 4), 2852(± 2), and 2921(± 4) cm^{-1} , typical of polyazines. In most of the compounds, there are also prominent absorptions in the 3200–3400 cm^{-1} region, indicative of water of hydration and/or NH_2 end groups. In the dimers, absorption bands are also found near 1700 cm^{-1} arising from the carbonyl end group. In some of the polymers, weak bands were also found near 1700 cm^{-1} , indicating the presence of carbonyl end groups. All of the compounds also have sharp peaks at 1084 and 771(± 1) cm^{-1} that are due to the PF_6^- counterions.

NMR Spectroscopy. The ^1H NMR spectra for the dimers and the polymer are quite different from either of the constituent monomers. Strong resonances are found at 1.24, 1.75, and 1.84 ppm, a broad range of bands are observed between 7.2 and 9.0 ppm, and weaker features are found

near 0.86 and 2.08 ppm. The weak absorptions are assigned to methyl groups on polymer or dimer termini based on the assignments known for $[\text{Ru}(\text{bpy})_2\text{BADA}]^{2+}$ where the ketone methyl group is found at 2.07 ppm and the adjacent imine methyl group resonates at 0.81 ppm.⁶⁵ The broad and unresolved bands in the aromatic region arise from the bpy ligands. These bands are not sufficiently resolved for a detailed assignment, but the pattern is consistent with coordinated 2,2'-bipyridine. Finally, the remaining strong bands are assigned to methyl groups on the bridging azine linkage. The peak at 1.24 ppm is assigned to the methyl group adjacent to the metal-chelate ring because the relative intensity of this peak decreases as the length of the bridging group increases. The peaks at 1.75 and 1.84 ppm are assigned to methyl groups along the bridging azine linker. The relative intensity of these two features changes in an unsystematic pattern as the length of the bridge increases, indicating that the degree of nonplanarity of the azine units varies for each compound. The resonances for the methyl groups on the diimine chelate ring are hidden under the solvent peak in $\text{DMSO}-d_6$ at 2.5 ppm except for Dimer2 where the chelate ring resonance is observed at 2.46 ppm. For the polymers, the degree of polymerization (DP) was estimated using the integration of the entire methyl region compared to the entire bpy region. This gave DP values typically of 4–5, depending upon the sample, indicating molecular weights on the order of 4000–5000.

Electrochemistry. Cyclic voltammetry experiments were run for each of the dimers and polymers, and all of the materials gave similar results. Reductions of the complexes, which were typically around -0.8 V (vs Ag/AgCl), were ill defined and unresolved. The observed oxidation potentials are listed in Table 1. Three oxidations were observed, near 0.5, 0.8, and 1.5 V, with the exception of Poly3, which only showed two oxidation peaks at 0.59 and 1.55 V. If scans were reversed at 1 V, then the 0.5 and 0.8 V oxidations were

Table 1. Electrochemical and Spectroscopic Parameters for the Dimers and Polymers

compound	E° (V, vs Ag/AgCl)	λ_{\max} (nm) (ϵ M ⁻¹ cm ⁻¹)	ω (fit, cm ⁻¹)	λ_{\max} , IT (nm)	f_{ox} (IT max)
[Ru(bpy) ₂ BDDH] ²⁺ (ref 66)	1.11 1.51	413 (16500)	23480 24620		
[Ru(bpy) ₂ BADA] ²⁺ (ref 66)	1.22 1.52	442 (7640)	22500 22580		
Dimer2	0.52 0.82	438 (12300)	18220 22720		
Dimer3	1.53 (irrev) 0.57 0.81	444 (6500)	23230 19680 21180		
Dimer4	1.48 (irrev) 0.57 0.81	446 (17000)	22630 19530 22400		
Dimer5	1.48 (irrev) 0.50 0.80	439 (12000)	22930 20840 22960		
Dimer6	1.49 (irrev) 0.49 0.81	448 (5100)	25490 20610 22050		
Poly1	1.55 (irrev) 0.49 0.82	436 (880)	23310 19680 21870	14120	0.021
Poly2	1.55 (irrev) 0.58 0.81	441 (7300)	22810 19400 22710	13720	0.057
Poly3	1.46 (irrev) 0.59	462 (4100)	24370 16600 18880	6530	0.25
Poly4	1.55 (irrev) 0.57 0.80	435 (7700)	21100 19680 22650	14140	0.18
Poly5	1.47 (irrev) 0.55 0.80	443 (12000)	24100 18100 19870	13930	0.26
Poly6	1.48 (irrev) 0.48 0.82	447 (3100)	22360 19640 21300	13810	0.16
Poly7	1.47 (irrev) 0.46 0.74	447 (4600)	22620 20840 23010		
	1.48 (irrev)				

quasireversible with peak-to-peak separations around 50 mV. When scans were run to higher potentials, the oxidation at 1.5 V was irreversible and induced irreversibility in the lower potential peaks, as well. The well-separated peaks observed in the forward scan become a broad single peak in the reverse scan. Examples of this are shown in Figure 1. In comparison to other ruthenium polypyridyl complexes, the oxidation at 1.5 V is assigned to the metal site, Ru²⁺ to Ru³⁺, while the lower potentials are assigned to ligand processes. Oxidation of the metal apparently also induces a reaction on the oxidized ligand. In comparison, the monomer complexes [Ru(bpy)₂BDDH]²⁺ and [Ru(bpy)₂BADA]²⁺ only have two irreversible oxidations, a ligand oxidation at 1.11 and 1.22 V, respectively, and a metal-centered oxidation at 1.51 and 1.52 V, respectively.⁶⁶ Many of the voltammograms had a small, irreversible peak near 1.2 V. While this could be associated with oxidation of end groups, it was established that this wave was due to water of hydration since the peak could be increased by addition of water to the solution.

Electronic Spectroscopy. The visible spectra of the dimers and polymers are dominated by MLCT transitions around 440 nm, typical of Ru²⁺ diimine complexes, as shown by the examples in Figure 2. As given in Table 1, the λ_{\max} are

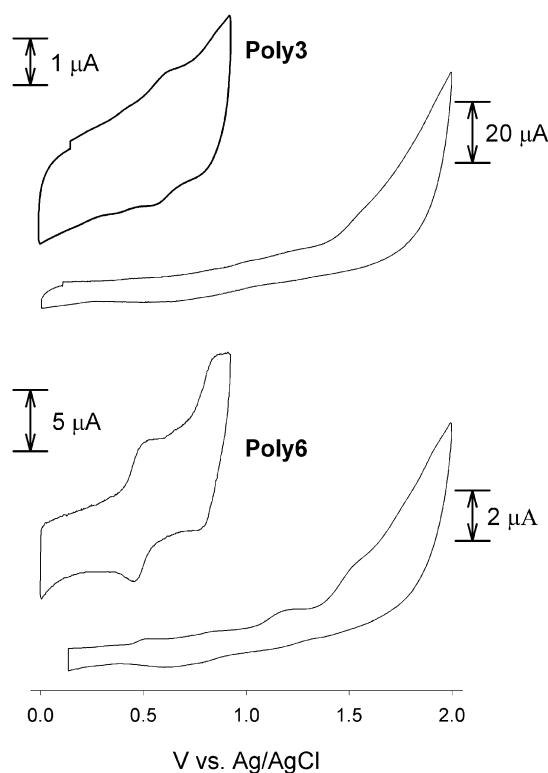


Figure 1. Cyclic voltammograms for Poly3 and Poly6 in 0.10 M LiClO₄ in acetonitrile at 25 °C and a sweep rate of 100 mV/s. Note the change in reversibility of the low potential peaks when the switching potential changes from 1 to 2 V. The feature at 1.2 V is due to water of hydration.

similar for all of the dimers and polymers (except Poly3) and are comparable to λ_{\max} found for the monomer [Ru(bpy)₂BADA]²⁺ but red shifted compared to [Ru(bpy)₂BDDH]²⁺. Poly3, which has $\lambda_{\max} = 462$ nm, is significantly shifted to lower energy from the other compounds. Other than the anomaly with Poly3, there is no apparent trend in the absorption maxima in either the dimers or polymers. The absorption data were deconvoluted into Gaussian line shapes, and these results are given in Table 1. Except for Poly7, each of the dimers and polymers gives rise to three peaks in the MLCT region. This is in contrast to the monomers [Ru(bpy)₂BDDH]²⁺ and [Ru(bpy)₂BADA]²⁺ where the MLCT absorption is accounted for by two peaks.⁶⁶

None of the dimers or polymers were found to have any emission in acetonitrile solution at room temperature. This is similar to the [Ru(bpy)₂BADA]²⁺ monomer, which also is nonemissive at room temperature⁶⁶ but different from [Ru(bpy)₂BDDH]²⁺, which has a weak luminescence. The flexible and conformationally labile polyazine ligands are likely responsible for rapid nonradiative decay of the MLCT excited state.

Oxidation of Poly1 through Poly6 in solution using Ce⁴⁺ gave rise to a peak in the NIR region consistent with an IT transition. None of the dimers gave an IT peak nor did Poly7. As the reduced solution is titrated with Ce⁴⁺, the IT peak becomes more intense and then reduces in intensity and then eventually disappears. The titration spectra showed isosbestic points when the mole ratio of the oxidant was small, indicating that there are probably only two absorbing species in solution at low oxidation levels. This indicates that even

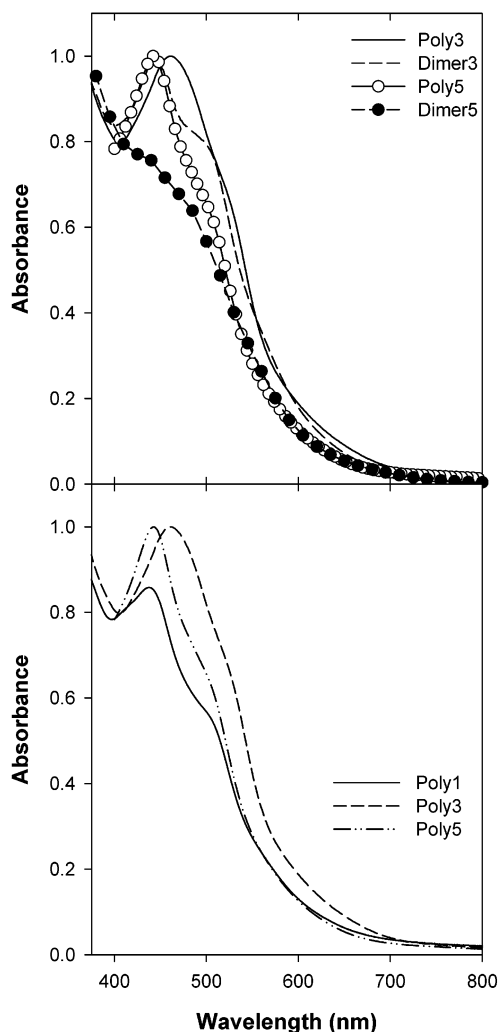


Figure 2. Visible spectra for Poly1, Poly3, Poly5, Dimer3, and Dimer5 in acetonitrile at 25 °C. The top graph compares the spectra of dimers to those of the corresponding polymers, and the bottom graph compares the spectra of different polymers.

though the Ce^{4+} ion is thermodynamically capable of oxidizing either the Ru^{2+} or the polyazine ligand, only one site is losing an electron, presumably for kinetic reasons. Examples of the spectroscopic titration are shown in Figure 3 and the IT peak maxima are listed in Table 1. The fraction of monomer sites oxidized, $f_{\text{ox}} = [\text{Ce}^{4+}]/[\text{Ru}^{2+}]$, to reach the maximum intensity for the IT peak was always below the expected value of $f_{\text{ox}} = 0.5$. These values are also given in Table 1.

Computations. PM3 and DFT calculations were performed on Dimer1, Dimer2, and Dimer3 to better help us understand the experimental observations. Geometries were optimized using PM3 for each dimer in the 4+, 5+, and 6+ states. These geometries were then used as input for the DFT calculations to find the electronic structure and charge distribution for each of the model compounds. For comparison purposes, we also used the same procedure for the monomer $[\text{Ru}(\text{bpy})_2\text{BADA}]^{2+}$ and its first two oxidized states, $[\text{Ru}(\text{bpy})_2\text{BADA}]^{3+}$ and $[\text{Ru}(\text{bpy})_2\text{BADA}]^{4+}$. The results for the bond lengths and dihedral angles along the polyazine backbone and the charge and spin density distributions are given in Supporting Information, Tables 1–4. The

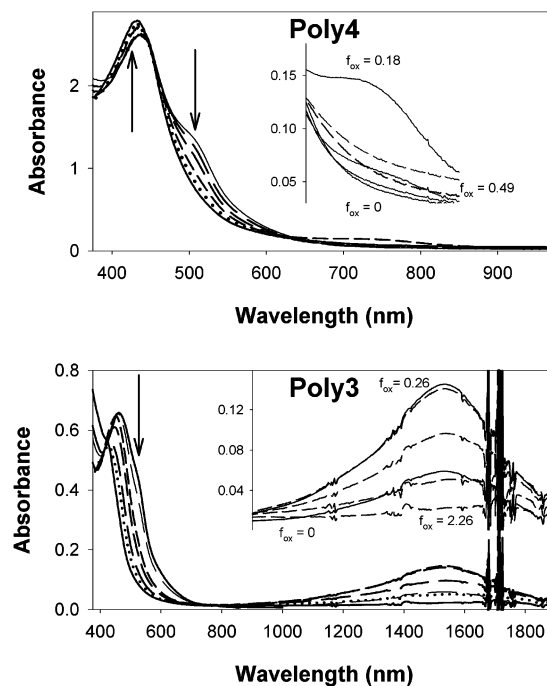


Figure 3. Spectral changes observed during the oxidation of Poly4 (top) and Poly3 (bottom) during oxidation by Ce^{4+} in the visible and NIR region. The insets show an enlarged view of the IT band that is formed and then lost during the titration.

calculations predict that the fully reduced dimers are significantly twisted along the polyazine backbone, with dihedral angles around the single bonds ranging from 70 to 80°. The structures found are shown in Figure 4 using a view down the Ru–Ru axis to emphasize the twisting of polyazine ligand induced by the nonplanarity of the polymer ligand. When the compounds are oxidized, in general, the N–N and C–C bonds become shorter and the C=N bonds become longer.

Oxidation also induces changes in the dihedral angles, usually with a noticeable flattening of one of the dihedral angles about an N–N bond. The changes in the charge and spin densities in $[\text{Ru}(\text{bpy})_2\text{BADA}]^{2+}$, dimer1⁴⁺, and dimer2⁴⁺ suggest that the first oxidation is mixed between the ruthenium atoms and the polyazine ligand, consistent with the electrochemical assignment, and that the second oxidation is located primarily on the Ru atoms, in conflict with the previous assignment. In contrast, the calculations imply that both of the first two oxidations occur on the polyazine in dimer3⁴⁺. In all cases, there is significant mixing of the ruthenium and ligand orbitals.

The energy level diagrams from the DFT calculations for the reduced and first oxidized states for $[\text{Ru}(\text{bpy})_2\text{BADA}]^{2+}$, Dimer1, Dimer2, and Dimer3 are shown in Figure 5. In the monomer the highest occupied orbitals are mainly d character, while for each of the dimers the HOMOs are mainly ligand character. Upon oxidation, all of the compounds lead to ligand oxidation, consistent with the experimental observations. In each of the dimers, the spin density indicates that the oxidation is delocalized over both ruthenium sites, although this may be an artifact of the B3LYP functional.^{74,75} In Dimer1 and Dimer2 the relative energies of the d orbitals

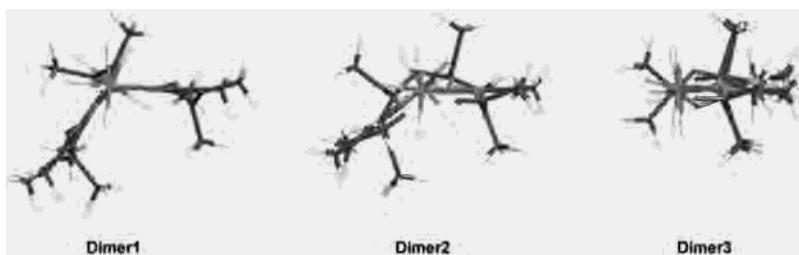


Figure 4. PM3 calculated structures of Dimer1⁴⁺, Dimer2⁴⁺, and Dimer3⁴⁺ viewed along the Ru–Ru axis. The bipyridine ligands have been omitted for clarity. Notice the developing helical nature of Dimer1 and Dimer2 but the coplanarity of the metalocyclic rings in Dimer3.

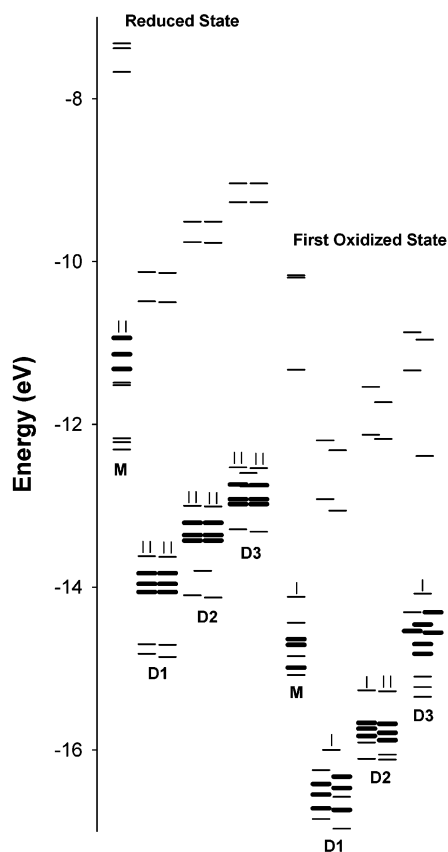


Figure 5. Energy level diagrams for [Ru(bpy)₂BADA]²⁺ (M), Dimer1⁴⁺ (D1), Dimer2⁴⁺ (D2), and Dimer3⁴⁺ (D3) and their respective first oxidized states. The energies were found using DFT calculations on structures optimized using the PM3 method.

on each Ru site are nearly degenerate for both the reduced and first oxidized state. In contrast, there is a significantly larger scrambling of orbital energies for Dimer3.

Discussion

The polymers studied in this work are best thought of as organic polymer systems with metal containing substituent groups. The metal–ligand groups strongly affect the polymer solubility, oxidation reaction chemistry, and electronic structure. The ruthenium ions have a marked, long-range effect on the properties of the polyazine ligand, as evidenced by the NMR spectra and the electrochemical potentials.

The NMR spectra show that the resonances for the CH₃ groups on the bridge never approach the chemical shifts

found in the uncomplexed oligoazines. Even in Poly7, where the Ru ions are separated by more than 30 Å, the observed chemical shifts are similar to those found in Poly1, where the interior distance is less than 10 Å. Thus, the Ru²⁺ ions are able to influence the electronic structure of the polyazine ligand for distances of at least 15 Å. Further, since there is no gradual change of chemical shifts with increasing length of bridging ligand, the influence of the ruthenium ions on the bridging ligand cannot be simply due to a charge effect, since this would wane, probably following a simple power law. Thus, the conclusion drawn from the NMR spectra is that the Ru²⁺ ions are strongly coupled to the azine ligand system, which allows the possibility that the metal ions are weakly coupled to each other over long distances.

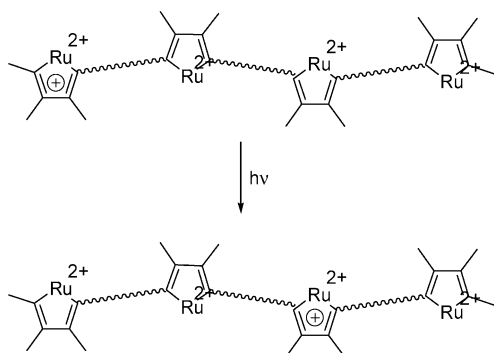
The electrochemical potentials support this conclusion. The ligand oxidation is lower in the multimetal complexes than in the monometal complexes and split into two peaks (except for Poly3). The first oxidation is bridge length dependent but is not monotonically changing as the bridge length increases. If adjacent metal sites are coupled to each other, then a consistent assignment of the oxidation potentials can be made. The first oxidation is ligand centered and is primarily located near the metalocyclic ring, but may be delocalized over two monomer sites. The second oxidation also occurs near a metalocyclic ring but at the site adjacent to the first oxidation. Both of these oxidations are reversible if the applied potential is kept below 1 V. At more positive voltages, the Ru²⁺ sites are formally oxidized to Ru³⁺. This causes a change in the structure of the oxidized metalocyclic ring, perhaps pushing the oxidation into the center of the bridge. This changes the potential for reduction of the Ru³⁺ and the ligand, accounting for the irreversibility, and likely decomposition of the initial compound. Poly3 only shows a single ligand oxidation, which may be due to the similar geometry found at each metal site in this polymer.

The anomalous low energy MLCT band found for Poly3 is probably a consequence of the coplanar geometry of the adjacent ruthenium metalocycle sites along the polyazine chain. Since Dimer3 does not show unusual MLCT behavior, this suggests that the excited states in Poly3 may be delocalized over several repeat units, which accounts for the low energy absorption. The spectroscopic anomaly found in Poly3 extends to the IT band found in the oxidized state, which is at much lower energy than any of the other polymers. In fact, though, the spectroscopic behavior of the oxidized state of all of the materials studied here is unusual. For the dimers, upon oxidation there is no band found that

(74) Bally, T.; Sastry, G. N. *J. Phys. Chem. A* **1997**, *101A*, 7923.

(75) Zhang, Y. Yang, W. *J. Chem. Phys.* **1998**, *109*, 2604.

Scheme 3

**Table 2.** IT Band Peak Maxima, Linewidths, Molar Absorptivity, and Derived Intervalence Coupling^a

polymer	ω_{max} (cm ⁻¹)	$\Delta\omega_{1/2}$ (cm ⁻¹)	ϵ_{max} (M ⁻¹ cm ⁻¹)	V_{ab} (cm ⁻¹)
Poly1	13700	1400	88	46
Poly2	13600	1060	610	110
Poly3	6510	540	910	63
Poly4	13500	850	410	67
Poly5	13300	810	530	60
Poly6	13500	1310	81	22

^a The band maxima and line widths were found by plotting A/ω vs ω and fitting to a Gaussian peak shape. The molar absorptivities are uncorrected. The intervalence coupling values were found using the Hush formula, as described in text.

can be attributed to a $[\text{Ru}^{2+}, \text{Ru}^{3+}] \rightarrow [\text{Ru}^{3+}, \text{Ru}^{2+}]$ IT-type transition. Since the first oxidation is ligand-based, this may not be surprising. However, the polymers do exhibit an absorption band typical of an IT but must be a ligand–ligand centered excitation. This IT is also unusual because the maximum absorption is found at low oxidation levels, $f_{\text{ox}} \sim 0.25$. The IT band might be assigned to a subband gap polaron transition in these conjugated systems, but a polaron is expected to display three peaks, which is not observed here. Further, upon increased oxidation a polaron is expected to evolve into a bipolaron, which should have two subband gap absorptions and this is also not observed. Thus, we assign the IT peak to a dimer-to-dimer ligand–ligand transition for each polymer, as depicted in Scheme 3.

This is consistent with the electrochemistry, which implies that neighboring repeat units are coupled. This also explains why the IT maximizes at $f_{\text{ox}} \sim 0.25$ – four repeat units are required for the transition to occur. The much lower f_{ox} for the IT maximum shown in Table 1 for Poly1 and Poly2 probably arise because these two materials contain a larger fraction of shorter (DP < 4) chains.

We calculated the donor–acceptor coupling using the standard Hush formula, $V_{\text{Hush}} = 0.0205\sqrt{\omega_{\text{max}}\Delta\omega_{1/2}\epsilon_{\text{max}}}/r$, using the metal–metal distance between the donor and acceptor sites^{21–25} and correcting for the dihedral angle between metal sites, $V_{\text{ab}} = \cos(\theta)V_{\text{Hush}}$,⁷⁶ using the angles and distances determined from the PM3 calculations. The results are given in Table 2. The coupling constants are small. If an exponential decay is assumed, then a decay constant of 0.040 Å⁻¹ is found (albeit with a large scatter). The

distances and angles used in this calculation are rough estimates, at best, so that the coupling constants that are reported have large errors. However, the trends in V_{ab} indicate that, despite the spectroscopic dissimilarity to the other compounds, the coupling constant for Poly3 is similar to all of the other mixed-valence polymers. This indicates that the relatively low energy peak maximum in Poly3 arises for reasons not associated with the donor–acceptor coupling.

Conclusion

A series of polyazines and dimer model compounds containing $[\text{Ru}(\text{bpy})_2]^{2+}$ complexes at controlled sites along the polymer chain were synthesized. The C=N–N=C bonds are significantly twisted so that the relative orientation of the metallocycle sites are not coplanar and depends on the number of azine repeat units between metal sites. The NMR spectra indicated that the metal sites had a long-range influence into the polymer backbone up to at least 15 Å. The cyclic voltammograms of the materials studied showed two low potential features that were attributed to oxidation of the ligand near the metal sites, which was also consistent with DFT calculations. The first oxidized state showed a spectroscopic transition with behavior similar to the familiar IT transition found in many diruthenium complexes. However, the IT absorption was found only in the polymers and not in the dimers, implying that the transition requires more than two repeat units. Thus, the IT was assigned to a ligand-centered donor–acceptor transition spanning two metallocyclic units. With this assignment, the coupling constant between the donor and acceptor sites was found to be small for all of the polymers but with only a slight decay as a function of distance up to the conjugation length of the bridging unit.

Thus, despite the presence of the transition metal complex at each repeat unit, the materials studied here behave as organic polymers. The $\text{Ru}(\text{bpy})_2^{2+}$ complexes serve as substituent groups that strongly interact with the delocalized polymer backbone. The cationic substituent groups promote solubility in water and determine the oxidation site of the polymer to be at the ligand. In contrast, the interaction between repeat units is set by the polymer ligand conformation, which is twisted at the azine linkages and leads to small coupling constants.

In future studies, we plan to investigate the solid-state characteristics of these materials. In particular, the spectroscopic and charge transport properties of the polymers should prove to be interesting. Since there appears to be at least some coupling between oxidized and unoxidized sites, reasonable electrical conductivity may be possible.

Acknowledgment. We thank the National Science Foundation (Grant 9729819) for support of this work.

Supporting Information Available: Tables with bond lengths, dihedral angles, atomic charges, spin densities, and total energies found from PM3 and DFT calculations for $[\text{Ru}(\text{bpy})_2\text{BADA}]^{n+}$, Dimer1ⁿ⁺, Dimer2ⁿ⁺, and Dimer3ⁿ⁺. This material is available free of charge via the Internet at <http://pubs.acs.org>.

(76) Davis, W. B.; Ratner, M. A.; Wasielewski, M. R. *J. Am. Chem. Soc.*, **2001**, *123*, 7877.